CSR-IMMUNE Arc COMPRESSORS FOR RECIRCULATING ACCELERATORS DRIVING HIGH BRIGHTNESS ELECTRON BEAMS

S. Di Mitri†, M. Cornacchia, Elettra – Sincrotrone Trieste S.C.p.A., Basovizza, Trieste I-34149

Abstract

The advent of short electron bunches in high brightness linear accelerators has raised the awareness of the accelerator community to the degradation of the beam transverse emittance by coherent synchrotron radiation (CSR) emitted in magnetic bunch length compressors, transfer lines and turnaround arcs. We reformulate the concept of CSR-driven beam optics balance, and apply it to the general case of varying bunch length in an achromatic cell. The dependence of the CSR-perturbed emittance to beam optics, mean energy, and bunch charge is shown. The analytical findings are compared with particle tracking results. Practical considerations on CSR-induced energy loss and nonlinear particle dynamics are included. As a result, we identify the range of parameters that allows feasibility of an arc compressor in a recirculating accelerator driving, for example, a free electron laser or a linear collider.

INTRODUCTION

In spite of the relatively high beam rigidity from hundreds of MeV up to multi-GeV energies, the electron beam energy-normalized projected emittance may be degraded in the bending plane at the ~1 μm rad level and above, when the beam is bent in dipole magnet-chicanes that act as bunch length compressors [1–4], in multi-bend transfer lines [5] and in turnaround arcs [6–11]. Initially thought for a constant bunch length along the line [12], a specific linear optics design has recently been revisited to minimize [5] or even cancel [13] the emittance disruption in double bend achromatic (DBA) lines, and then in a periodic [14] and a non-periodic arc [15], in which the bunch length is notably compressed. Turnaround arcs have been considered as magnetic bunch length compressors for energy-recovery linac (ERL) designs, in the 0.1–1 GeV energy range [6–11]. In [8,9] some degree of optics control was exercised in order to minimize the CSR effect following the theoretical prescriptions given in [16], but in all cases the CSR effect was effectively suppressed by limiting the bunch charge below 0.15 nC. To date, when arcs are included in the accelerator geometry, bunch length is kept constant through them by isochronous paths, or lengthened before entering the arc (CSR effect is weaker for longer bunches), and re-compressed at its end. In this article, we follow [17] and recall the range of validity of the linear optics analysis and investigate the robustness of the proposed arc compressor lattice for a realistic range of beam parameters, where a normalized emittance at the arc's end at the 0.1 μm rad level is promised, for compression factors of up to ~45, applied to a 0.5 nC beam, at 2.4 GeV.

† simone.dimitri@elettra.eu

LINEAR OPTICS FORMALISM

The periodic, achromatic 180 deg arc compressor introduced in [14] is made of 6 identical DBA cells. The single DBA magnetic lattice and its periodic optics solution is shown in Fig.1. We assume optics symmetry w.r.t. the DBA central axis, which implies π betatron phase advance (in the bending plane) between the dipoles [18], and expand the trigonometric terms up to the 3rd order in the bending angle, θ<<1. Following the mathematics in [17], we calculate the expression of the single particle Courant-Snyder (C-S) invariant at the end of the second dipole magnet for arbitrary C-S parameters in the dipoles, by considering a dependence of the CSR kick factor on the rms bunch length k ~ 1/σz4/3, so that k2 = k1×C4/3, where C is the bunch length compression factor through the DBA cell. The particle invariant is minimized by the following C-S parameters in the second dipoles [17]:

$$\alpha_{2,opt} = -\frac{\beta_2}{\left(\frac{l_b}{6}\right)}\frac{\left(C^{4/3}+1\right)}{\left|C^{4/3}-3\right|}, \qquad (1)$$

$$\beta_{2,opt} = \left(\frac{l_b}{6}\right)\frac{\sqrt{\left(C^{4/3}-1\right)^2+\alpha_2^2\left(C^{4/3}-3\right)^2}}{\left(C^{4/3}+1\right)}$$

We notice that a solution with $\alpha_2 = 0$, e.g. adopted in [14], does not minimize J_3 in absolute sense, although it may be practical from the optics design point of view.

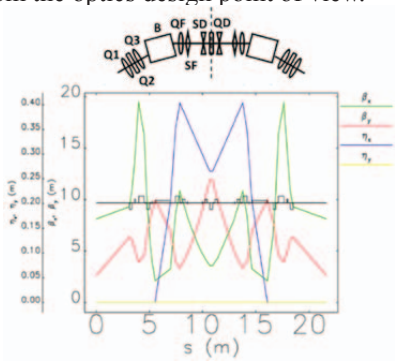

Figure 1: Linear optics functions and DBA cell layout including dipole magnets (B), focusing (QF, Q1 and Q3) and defocusing (QD, Q2) quadrupole magnets, focusing (SF) and defocusing sextupole magnets (SD). Copyright of Elsevier (2016) [17].

LINEAR COMPRESSION FACTOR

The linear compression factor is defined by $C=1/|1+hR_{56}|$, where R_{56} is the transfer matrix element of the DBA cell, identical in all cells, and h is the incoming linear energy chirp, h=dE/(Edz), E being the beam mean energy. Bunch length compression is achieved as far as the energy spread correlated along the bunch, typically imparted to the beam by an upstream RF section running

far from the accelerating crest, is much larger than the uncorrelated energy spread. While σ_δ does not change substantially during the compression process, σ_z clearly shortens with C, that is h increases along the arc, and C so does. In summary, the local compression factor, C^{loc}, and that cumulated through the lattice, C^{tot}, depends on the cell number [17]:

$$C_i^{loc} = \frac{1}{|1 + C_{i-1} h_{i-1} R_{56}|}, \quad i = 1,\ldots,6 \qquad (2)$$

$$C_j^{tot} = \prod_{i=1}^{j} \frac{1}{|1 + C_{i-1} h_{i-1} R_{56}|}, \quad j = 1,\ldots,6$$

C^{tot} grows nonlinearly with the s-coordinate along the arc, and β_2 should be tuned accordingly in each DBA, in order to minimize the CSR emittance (see Eq.1). Since the CSR effect is larger for shorter bunches, we might relax the condition on β_2 in the first few cells, where the bunch is longer, while ensuring optimum tuning in the last ones.

PROJECTED EMITTANCE GROWTH

We assume that the CSR emittance in each cell sums in quadrature to the total emittance of the incoming beam, whereas normalized emittance in the *i-th* cell is estimated by means of the "sigma matrix formalism" [19] and turns out to be:

$$\varepsilon_{n,i} \cong \sqrt{\varepsilon_{n,i-1}^2 + \varepsilon_{n,i-1} \beta_i \gamma_i J_i} \qquad (3)$$

β_i and γ_i are the usual relativistic Lorenz factors, J_i is particle's C-S invariant and we have to evaluate it with the prescription $C=C_i^{loc}$ according to Eq.2. Figure 2-left plot shows C_i^{loc}, $\beta_{x,opt}$ and γJ_i along the arc, for the beam parameters listed in Tab.1 (henceforth, β_x refers to the betatron function in the dipole magnets). Figure 1-right plot compares J_i evaluated for $\beta_{x,opt}$ as in the left plot, to that for an identical value of β_x in all the dipoles.

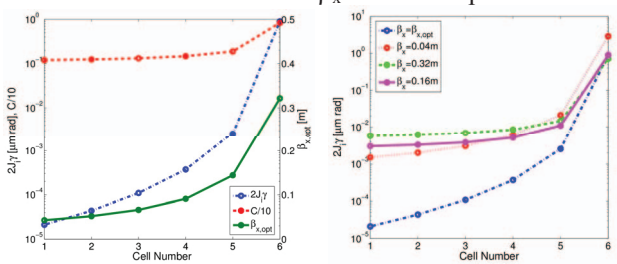

Figure 2: Left: local value of C/10 and of $\beta_{x,opt}$ in the dipoles vs. arc cell number. Right: the local value of the $\beta_{x,opt}$ is compared with its value evaluated for an identical β_x value in all the dipoles. Copyright of Elsevier (2016) [17].

The arc compressor performance is investigated for different beam mean energies in Fig.3. The magnets' normalized strengths are kept fixed in order to provide the same optics for all energies. The quadratic difference of the final projected emittance and the unperturbed one is shown for beam charges of 0.1, 0.3 and 0.5 nC. Particle tracking results are compared with the analytical prediction of Eq.3. The magnets' length were optimized for the maximum beam energy of 2.4 GeV, and therefore Fig.3 shows a scenario which is as more pessimistic as the beam energy is lower. For the analytical case, the CSR-induced energy spread was evaluated according to the steady-state emission of a uniform charge distribution [20].

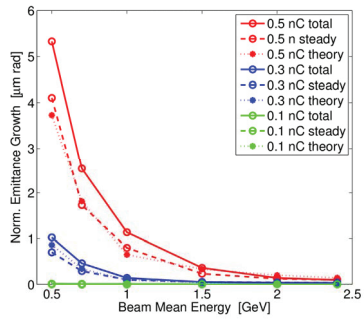

Figure 3: The normalized emittance growth is the quadratic difference (under square root) of the final projected normalized emittance and the initial one (rms values). Theoretical predictions (dotted lines) are from Eq.3, for steady-state CSR emission. Particle tracking results are for steady-state emission (dashed lines), and including transient CSR field at the dipoles' edges, and in drift sections (solid lines). The arc lattice is made of 6 consecutive cells, whose unit is shown in Fig.1. The optics is the same for all beam charges and energies. Copyright of Elsevier (2016). Elsevier (2016) [17].

Table 1: Main Beam and Arc Compressor Parameters

Parameter	Value	Units
Energy	2.4	GeV
Charge	0.5	nC
Initial Bunch Length, RMS	900	μm
Correl. Energy Spread, RMS	0.4	%
R_{56} per DBA Cell	35	m
		m
Number of DBA Cells	6	
Total Compression Factor	45	
Final Peak Current	2000	A

NONLINEAR OPTICS

The bunch length compression process is linearized through the arc with the help of 4 families of sextupole magnets, 24 magnets in total. In fact, linear compression is achieved as long as $|T_{566}|\sigma_{\delta,0} << |R_{56}|$ through the arc. In addition, second and higher order energy chirp has to be small with respect to the linear one. While T_{566} can be controlled, *e.g.*, with an appropriate number and strength of sextupole magnets, a nonlinear energy chirp is realistically present in the beam's longitudinal phase space: at the entrance of the arc compressor due to upstream RF curvature, and developing along the arc because of the nonlinear energy correlation established by CSR along the bunch. Then, a non-zero T_{566} can be used to linearize the nonlinear chirp, the actual value of T_{566} (typically in the cm range) depending on the specific charge distribution (i.e., CSR strength).

The single sextupole aberration can be analytically estimated through the sigma matrix formalism. The sextupole aberration is excited by a kick $\langle \Delta u'^2 \rangle = (k_2 l_s)^2 \langle u^2 \rangle^2$, with $k_2 l_s$ the integrated normalized sextupole strength in m^{-2}, $\langle u^2 \rangle = \beta \varepsilon_0$ for the geometric aberration, and $\langle u^2 \rangle = \eta_x^2 \sigma_\delta^2$ for the chromatic one. We consider the scenario in which the final relative emittance growth is given by the largest sextupole's contribution folded by the square root of the number of sextupoles in the lattice. With the beam parameters listed in Tab.1 and the optics depicted in Fig.1, the total relative emittance growth from geometric aberrations is smaller than 0.01%, while that due to chromatic aberrations is above 100%. This explains the modulation of the projected emittance along the arc shown in Fig.4. The effect of chromatic aberrations was eventually minimzed by a numerical optimization of the sextupole strengths, and by profiting of the betatron phase advance between the magnets.

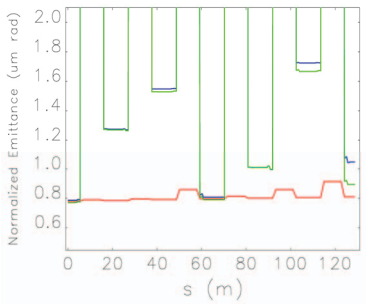

Figure 4: Projected rms normalized horizontal emittance along the arc; beam parameters as in Tab.1. The emittance evolution is shown in the presence of ISR-only for the fully compressed beam (red), with the addition of compression and optical aberrations (green) and with the further addition of CSR (blue). Copyright of Elsevier (2016) [17].

CSR-INDUCED ENERGY LOSS

The 1-D steady-state theory of CSR emission from a Gaussian bunch allows an estimation of the CSR-induced mean energy loss per dipole magnet [21], $<\delta_{CSR}>=-0.3505\times r_e Q/(e\gamma\rho^{2/3}\sigma_z^{4/3})$. A more realistic evaluation from particle tracking included the energy loss associated to the electrons-field interaction in drift regions. We found that a 0.5 nC charge beam may emit an average power of up to 60 W per mA of average current, at the repetition rate of 1 MHz. Most of the power is emitted in the last two cells of the arc. That power can produce heating and therefore requires cooling and a careful evaluation of the machine run duration to prevent vacuum pressure rise.

ERRATUM AND DISCUSSION

The C-S formalism in the presence of CSR chromatic kicks was first introduced in [5]. We notice however that Eqs. 3 and 4, and therefore their elaboration in Eq.5, were derived for a case which is not that one depicted in Fig.1, but for a phase advance of 2π in between the inner dipoles of the beam line. Everything else in the Letter is correct, and actually refers to the exact derivation of the expression of the CSR-induced particle invariant in the FERMI Spreader that was later on reported in Eq.3.8 of [22]. The correct expression for the final particle invariant is recalled here for Reader's convenience:

$$2J_7 = 2J_1 4\alpha_1^2 \left(1 - \sqrt{\frac{\beta_s}{\beta_1}}\right)^2 \equiv 2J_1 X_{17}, \qquad (4)$$

As correctly depicted in [22], Fig.4 in that work shows the superposition of experimental data to theoretical emittance growth, as a function of a quadrupole strength. For each strength, the relative phase advance between the two DBA cells is also shown. The emittance growth was evaluated analytically with Eq.6 in [22], where the phase advance between the two DBA was calculated with Elegant code [23] starting from the experimental set up of the beam line. Doing this, however, Eq.6 was evaluated by assuming that the Twiss parameters at the dipoles do *not* change as the phase advance is varied. Such an approximation is removed in Fig.3.2 of [1], where the dependence of the Twiss parameters at the dipoles of the second DBA on the phase advance is retained. In summary, Fig.3.2 of [1] shows a more accurate prediction of emittance growth than the one shown in Fig.4 of [22]. The two results, however, are close each other. Still, the methods, the results and the conclusions reported in [22] remain valid, and are not modified by this comment.

Strategies and formalisms were proposed before [12,24] and after [25,26] the work published in [22], for the cancellation of chromatic CSR kicks on the transverse emittance through linear optics elements in a locally isochronous beam line (i.e, bunch length is assumed to be the same at all points of CSR emission). Those works elaborate on, and somehow improve, the CSR kick minimization problem introduced in [27]. They all imply, however, a *symmetry* of the Twiss parameters *and* of the energy dispersion function, at the dipole magnets where CSR kick is generated. In [22], instead, a method is first introduced that allows cancellation of CSR kicks also when the Twiss parameters are *not symmetric* along the line (referred to as optics balance), and the phase advance between dipoles is arbitrary. For this reason, the formalism introduced in [22] offers in principle more general optics solutions, which reduce to those reported elsewhere for the case of symmetric optics set up. The optics balance concept was successively extended to the case of *non-isochronous* beam lines in [14,17] for symmetric optics set up.

REFERENCES

[1] T. Nakazato *et al., Phys. Rev. Letters* 63 (1989) 2433.

[2] H. Braun *et al., Phys. Rev. Letters* 84 (2000) 658.

[3] K.L.F. Bane *et al., Phys. Rev. Special Topics – Accel. Beams* 12, 030704 (2009).

[4] S. Di Mitri *et al., Phys. Rev. Special Topics – Accel. Beams* 15, 020701 (2012).

[5] S. Di Mitri, M. Cornacchia, and S. Spampinati, *Phys. Rev. Letters* 110, 014801 (2013).

[6] J. Wu *et al.*, "Coherent Synchrotron Radiation Analysis for the Photoinjected Energy Recovery Linac and UVFEL Projects at the NSLS", in Proc. of the 2001 Part. Accel. Conf., RPAH012, Chicago, IL, U.S.A., June 2001.

[7] P. Piot *et al., Phys. Rev. Special Topics – Accel. Beams* 6, 030702 (2003).

[8] M. Shimada *et al*., *Nucl. Instrum. Meth. Phys. Research*, Sect. A 575, (2007) 315.

[9] M. Borland and V. Sajaev, "Optimization of Lattice for an ERL Upgrade of the Advanced Photon Source", in Proc. of the 24th Linear Accel. Conf., Victoria, BC, Canada, September 2008, paper TUP023.

[10] G.H. Hoffstaetter and Y.H. Lau, *Phys. Rev. Special Topics – Accel. Beams* 11, 070701 (2008).

[11] S.V. Benson *et al.*, *Journal of Modern Optics* 58:16 (2011) 1438-1451.

[12] D. Douglas, JLAB-TN-98-012 (1998).

[13] Y. Jiao *et al., Phys. Rev. Special Topics – Accel. Beams* 17, 060701 (2014).

[14] S. Di Mitri, M. Cornacchia, *Europhys. Letters* 109, 62002 (2015).

[15] D. R. Douglas *et al.*, *Thomas Jefferson National Accelerator Facility Report* No. JLAB-ACP-14-1751 (2014), arXiv:1403.2318.

[16] R. Hajima, *Nucl. Instrum. Meth. Phys. Research*, Sect. A 528 (2004) 335.

[17] S. Di Mitri, *Nucl. Instrum. Meth. Phys. Research*, Sect. A 806 (2016) 184–192.

[18] A. Jackson, Part. Accel. 1987, 22, 111.

[19] A.W. Chao and M. Tigner, *Handbook of Accelerator Physics and Engineering*, World Scientific, Singapore, 3rd ed. (2006) 66.

[20] E.L. Saldin *et al. Nucl. Instrum. Meth. Phys. Research*, Sect. A 398 (1997) 373.

[21] M. Borland, *Phys. Rev. Special Topics – Accel. Beams* 14, 070701 (2001).

[22] S. Di Mitri and M. Cornacchia, *Physics Reports* 539 (2014) 1–48.

[23] M. Borland, *APS Tech Note* LS-207 (2000).

[24] P. Emma and R. Brinkmann, *SLAC-PUB*-7554 (1997).

[25] M. Venturini, *Nucl. Instrum. Meth. Phys. Research*, Sect. A 794 (2015) 109–112.

[26] M. Venturini, *Phys. Rev. Special Topics – Accel. Beams* 19, 064401 (2016).

[27] R. Hajima, J. *Appl. Phys*., 42 (2003) 974 – 976.